

Load Shedding in High-Integrated Wind Energy Power Systems Using Voltage Electrical Distance

Tung Giang Tran

Electrical and Electronics Department
HCMC University of Technology and Education
Ho Chi Minh City, Vietnam
giangtt@hcmute.edu.vn

Thai An Nguyen

Electrical and Electronics Department
Cao Thang Technical College
Ho Chi Minh City, Vietnam
nguyenthaian@caothang.edu.vn

Minh Vu Nguyen Hoang

HCMC University of Architecture
Ho Chi Minh City, Vietnam
vu.nguyenhoangminh@uah.edu.vn

Ngoc Au Nguyen

Electrical and Electronics Department
HCMC University of Technology and Education
Ho Chi Minh City, Vietnam
ngocau@hcmute.edu.vn

Tan Thien Tran

Electrical and Electronics Department
Cao Thang Technical College
Ho Chi Minh City, Vietnam
trantanthien@caothang.edu.vn

Received: 26 January 2022 | Revised: 16 February 2022 | Accepted: 27 February 2022

Abstract—This paper presents a load shedding method for power systems with high integration of wind energy, considering their frequency response. The minimum load shedding power needed to restore system frequency to operational limits can be determined by using the modified frequency response model along with secondary frequency control. The voltage electrical distance method can then be applied to appropriately distribute the shedding power to load buses. This method brings selectivity to the problem and minimizes the impact caused by load shedding. The proposed method was validated using simulations on the IEEE 37-bus test system with a modified wind power generator model.

Keywords—modified frequency response (FR) model; load shedding; voltage electrical distance (VED); secondary frequency control (SFC)

I. INTRODUCTION

The impact of the high integration of renewable energy, especially wind power plants, into classical power systems raises concerns [1-3]. Accordingly, stability issues should be studied and solved in power systems with high-integrated wind energy [4-7]. When a disturbance occurs in an integrated wind power system and causes a power imbalance, the problem is more serious if the generating capacity is less than the load demand, which requires the system to take measures to rebalance the power and stabilize its frequency [8-10]. In [11-13], virtual frequency controls with frequency response models of wind power systems were proposed to solve these stability

issues. However, when all control efforts have been taken and the frequency does not return to normal or within the allowable range, load shedding is the final option for preventing a system blackout. Load shedding methods based on priority for wind energy integration were proposed in [14]. Higher priority loads powered by reliable wind power were prevented from being shed under redundancy conditions, such as high load demand. A method to improve the recovery period of underfrequency transients was demonstrated in [15]. In the rate of frequency change for wind turbine power generation, virtual inertia control was applied under frequency contingency. The main focus of these studies was to evaluate the response of the system to disturbances and to consider wind power as a reliable energy source to prevent shedding loads.

An effective load shedding strategy requires the lowest amount of shedding power, which means that the system's control capabilities and Transmission System Operators' (TSOs) actions will provide the appropriate amount of additional power to the grid. This study deployed a modified Frequency Response (FR) model to analyze the frequency characteristics of the system considering wind energy, along with the secondary frequency control action of TSOs to obtain the minimum power for the load shedding strategy. The goal is to bring the system's frequency within normal operating limits and minimize the impact caused by load shedding. In addition, the voltage electrical distance method was used to distribute the shedding power and obtain selectivity. Furthermore, this study carried out simulations on the IEEE 37-bus system with a

Corresponding author: Tung Giang Tran

modified wind turbine model using the PowerWorld Simulation Platform to validate the effectiveness of the suggested method. The results were then analyzed and compared with a traditional load shedding method.

II. PRIMARY FREQUENCY CONTROL FOR WIND POWER

Assessing the controllability of Wind Turbine Generators (WTGs) when frequency disturbances occur is an important issue, especially with the high penetration of wind energy into the traditional power systems. Most WTGs are connected to the system entirely or partly through power converters, so the frequency control support in the form of the inertia of a WTG is negligible, even though there is a small amount of inertia reserve in its mechanical parts (blades, rotor generator). Therefore, using the Virtual Inertia (VI) controller, the kinetic energy stored in the WTG can be quickly released to adjust power and prevent a rapid drop in frequency when a large disturbance occurs. In addition, the droop controller helps to adjust the WTG's generation power to restore the system frequency within the normal operation range during the WTG's primary frequency control.

To generate more power for primary frequency control when there is a sudden increase in load demand, the WTG cannot operate in the Maximum Power Point (MPP) mode but needs to be deloaded to reserve a certain amount of power. Therefore, the pitch controller will enter the stage of deloading power from the WTG by mechanical power. The power system with high participation of WTG should apply this control method to get a good response to frequency disturbances. Therefore, the WTG's dynamic frequency control strategy applied in this study was based on VIC combined with the pitch angle deload control method. The control diagram is shown in Figure 1 of [16]. The parameters used in the primary frequency controller are: Δf and $\Delta\beta$ are the frequency and pitch angle deviations respectively, H_ω is the equivalent inertia time constant of the WTG, P_e , T_e , and T_m are the wind turbine's active output power, electrical, and mechanical torque respectively, k_b is the gain constant of the pitch controller, k_ω is the proportional gain, and R_ω is the droop constant.

A. Frequency Regulation Using Droop and Virtual Inertia Control

The additional electrical power control signal combined with the droop controller is expressed as:

$$\Delta P_{e1}(s) = -\left(\frac{1}{R_\omega} + k_\omega s\right) \Delta f(s) \quad (1)$$

B. The Pitch Angle-based Deloaded Control for WTGs

When deloading is neglected, WTG operates in the MPP mode with the mechanical and electromagnetic torque expressed as:

$$T_m = \frac{k_p C_p v^2}{\omega} \quad (2)$$

$$T_e = k_p \omega^2 \quad (3)$$

where C_p is the optimal power coefficient of the turbine depending on wind speed, rotor speed, and blade angle and k_p is the factor representing the maximum generating power at the rated condition. The deloaded power of the WTG is

accomplished by setting the blade angle β to a nonzero value, depending on the desired amount of power for reservation. And with the pitch angle-based deload controller, the blade angle will be regulated according to the frequency deviation [16].

III. FREQUENCY RESPONSE REPRESENTATION OF THE HIGH-INTEGRATED WIND ENERGY POWER SYSTEM

This section elaborates the system frequency response representation of the control method to evaluate the model's efficiency and determine the shedding power in the secondary frequency control. Using small-signal analysis, the reordered dynamic model of WTGs is presented as a small-signal linear transfer function. A modified FR model for a high-integrated wind energy power system will be obtained and the frequency response features will be evaluated. In addition, the stability of the closed-loop control system will be analyzed.

A. Dynamic Transfer Function of the WTG

The electromagnetic power P_e of the WTG is regulated through the primary controller (virtual inertia and droop controllers), while the mechanical power P_m is regulated by the pitch angle controller [16]. The total change of electromagnetic torque according to the frequency deviation using these control methods can be written as:

$$\Delta T_e(s) = -\left(\frac{1}{R_\omega} + k_\omega s\right) \Delta f(s) + 2k_p \omega \Delta \omega(s) \quad (4)$$

Using a small signal stability analysis and the linearization method, the change in mechanical torque ΔT_m due to the frequency deviation Δf and wind speed variation Δv can be given as:

$$\begin{aligned} \Delta T_m(s) &= \frac{\partial T_m}{\partial f} \Delta f(s) + \frac{\partial T_m}{\partial v} \Delta v(s) + \frac{\partial T_m}{\partial \omega} \Delta \omega(s) \\ &= \frac{k_p k_\beta k_b v^3}{\omega} \Delta f(s) + \left(\frac{3k_p C_{Pr} e f v^2}{\omega} - \frac{k_p k_c v^2 \lambda_{ref}}{\omega}\right) \Delta v(s) \\ &\quad + \left(\frac{k_p k_c v^2}{\omega} - \frac{k_p v^3 C_{Pr} e f}{\omega^2}\right) \Delta \omega(s) \end{aligned} \quad (5)$$

where $k_c = \frac{\partial C_p}{\partial \lambda}$ and $k_\beta = \frac{\partial C_p}{\partial \beta}$ will be considered constant in this study, based on the dynamic power characteristic of the turbines. The swing equation in the frequency domain is:

$$2H_\omega s \Delta \omega(s) = \Delta T_m(s) - \Delta T_e(s) \quad (6)$$

Joining (2), (3), and (4), the correlation relating the change of output power to frequency fluctuation can be expressed as:

$$\Delta P_e(s) = \frac{c}{bs+1} \Delta v(s) - \frac{a_2 s^2 + a_1 s + a_0}{bs+1} \Delta f(s) \quad (7)$$

where:

$$\begin{aligned} b &= \frac{\frac{2H_\omega \omega^2}{k_p}}{2\omega^3 + v^3 C_{Pr} e f - k_c \omega v^2} \\ c &= \frac{2k_p \omega^3 v^2 (3C_{Pr} e f - k_c \lambda_{ref})}{2\omega^3 + v^3 C_{Pr} e f - k_c \omega v^2} \\ a_2 &= \frac{\frac{2H_\omega \omega^2 k_\omega}{k_p}}{2\omega^3 + v^3 C_{Pr} e f - k_c \omega v^2} \end{aligned} \quad (8)$$

$$a_1 = \frac{\frac{2H\omega\omega^2}{R\omega k_p} - 2\omega^2 k_\omega}{2\omega^3 + v^3 C_{pr} e_f - k_C \omega v^2} + k_\omega$$

$$a_0 = -\frac{2\omega^2 \left(\frac{1}{R\omega} + k_p k_\beta k_b v^2 \right)}{2\omega^3 + v^3 C_{pr} e_f - k_C \omega v^2} + \frac{1}{R\omega}$$

B. The Modified FR Model for High-Integrated Wind Energy Power System

A widely used FR model was developed in [17] for a traditional power system, focusing on the response of thermoelectric generators. However, with the highly integrated large-scale wind energy into the power system and with the different characteristics from traditional generators, this FR model cannot be applied in this study. Based on the combination of the WTG's de-ordered dynamic model in (7) and the model proposed in [17], the modified FR model for high-integrated wind energy power systems was derived and is shown in Figure 1. The model in Figure 1 was applied to the system containing conventional and wind power generators. Therefore, the parameters of the model were modified using the equalization method presented in Section IV. T_R is the time constant, F_H is the generating power fraction of the thermoelectric generator, R is the characteristic constant of the governor (droop control), H is the system equivalent inertia time constant, D is the self-regulation coefficient of the load, and α is the participation factor of wind energy in the power system.

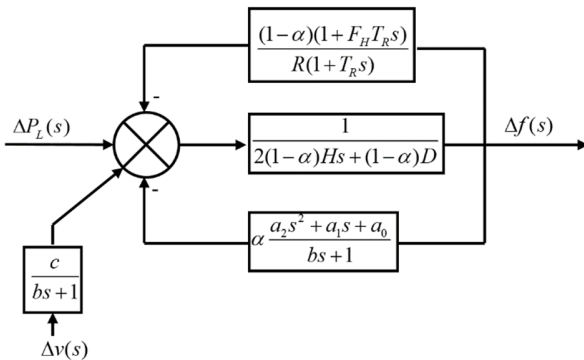


Fig. 1. The modified FR model for high-integrated wind energy power systems.

The input signals of the modified FR model are the fluctuations in load demand ΔP_L and in wind speed Δv , where the frequency variation Δf is the output of the proposed model. As seen in Figure 1, the modified FR output signal is influenced by the variation in both power demand and wind speed. In this study, the total power of the system is constant, and WTGs connected to the power grid are converted to the single-machine model. The superposition principle was used to analyze the impact of each input disturbance on the frequency variation of the system [18]. More specifically, when assessing the influence caused by the change in load demand to the frequency, the wind speed will be set as constant, and vice versa when evaluating the effect of wind speed variation. The transfer function of frequency deviation to fluctuations in load

and wind speed for the high-integrated wind energy power system is:

$$\Delta f(s) = \left[\frac{\Delta P_d}{s} + \frac{c}{bs+1} \frac{\Delta v_d}{s} \right] \frac{n_2 s^2 + n_1 s + n_0}{d_3 s^3 + d_2 s^2 + d_1 s + d_0} \quad (9)$$

$$n_0 = b T_R$$

$$n_1 = b + T_R$$

$$n_2 = 1$$

$$d_3 = \alpha a_2 T_R + 2(1 - \alpha) H b T_R$$

$$d_2 = (1 - \alpha) [2H(b + T_R) + D b T_R] + \frac{(1 - \alpha) F_H b T_R}{R} + \alpha (a_2 + a_1 T_R) \quad (10)$$

$$d_1 = (1 - \alpha) [2H + D(b + T_R)] + \frac{(1 - \alpha)(b + F_H T_R)}{R} + \alpha (a_1 + a_0 T_R)$$

$$d_0 = (1 - \alpha) D + (1 - \alpha) / R + \alpha a_0$$

where ΔP_d and Δv_d represent the disturbances in load demand and wind speed per unit. According to the initial/final value theory, the Initial Rate of Change of Frequency (IRCF) and the Steady-State Frequency Deviation (SSFD) of the system are obtained by:

$$IRCF = \lim_{t \rightarrow 0^+} \frac{d\Delta f(t)}{dt} = \lim_{s \rightarrow +\infty} s^2 \Delta f(s) \quad (11)$$

$$= \Delta P_d \frac{n_2}{d_2} = \frac{\Delta P_d}{\alpha k_\omega + 2(1 - \alpha) H}$$

$$SSFD = \lim_{t \rightarrow +\infty} \Delta f(t) = \lim_{s \rightarrow 0^+} s \Delta f(s)$$

$$= (\Delta P_d + c \Delta v_d) \frac{n_0}{d_0} \quad (12)$$

$$= \frac{\Delta P_d + c \Delta v_d}{(1 - \alpha) D + (1 - \alpha) / R + \alpha a_0}$$

The results from (11) and (12) were used to evaluate the frequency controllability of the power system with high wind energy penetration under disturbance conditions. The natural response of the system against disturbances can be defined as the primary control process of the system. The SSFD value will be the basis to decide whether or not to perform load shedding to stabilize the frequency within an allowable range.

IV. EQUIVALENT CONVERSION OF SYSTEM'S PARAMETERS

A. Equivalent Wind Power Generators Model

The uncertainty of wind power sources due to their dependence on weather and geometric conditions, as wind farms consist of many turbines, causes each turbine to behave inconsistently, leading to changes in the total generating power and the parameters of the whole wind farm. Therefore, having an equivalent conversion model of all or a part of the wind farm is essential to create homogeneity among the generating sources and to obtain the equivalent parameters used for the modified FR model. The method of equivalent transform proposed in [19] helps converting the wind farm into a single-generator model. The advantage of this method is that due to its simple implementation and equivalent model, it can be applied

to many problems. In addition, the equivalence method converts the wind farm into multiple generators and helps improving accuracy. A detailed equivalence method was proposed in [20] to analyze the location and wind speed data of each turbine to develop the wind farm model. The accuracy of the equivalent model is further enhanced by updating the data values. Due to the objective of this study, the equivalent method of a single-generator model will be used for simplicity.

B. Equivalence Method for System Parameters

To evaluate the system's frequency response to disturbances using the modified FR model, the parameters of a classical power plant such as the inertia time constant H and the self-regulating coefficient D are needed. The equivalence procedures of the parameters of a power system considering wind power sources were presented in [21] and are applied as:

$$H_{equ} = \frac{\sum_i^n H_i S_{b,i}}{\sum_i^n S_{b,i}} = \frac{\sum_i^n H_i S_{b,i}}{S_{tt}} \quad (13)$$

where H_{equ} and H_i are the equivalent and individual inertia time constants, S_{tt} is the total apparent power of the system, $S_{b,i}$ is the apparent power of the individual conventional generator, and n is the total conventional generating units. If m conventional generating units are replaced by WTGs with an equivalent amount of power, the system's inertia time constant is given as:

$$H'_{equ} = \frac{\sum_i^{n-m} H_i S_{b,i}}{\sum_i^{n-m} S_{b,i} + S_{WTG}} = (1 - \alpha) H_{equ} \quad (14)$$

V. DETERMINING MINIMUM LOAD SHEDDING POWER

A generator failure or severed load disturbance in a high-integrated wind energy power system causes an imbalance between generating power and load demand leading to a frequency deviation. In this case, the modified FR model shown in Figure 1 defines the response of the system, the initial rate of frequency change is calculated by (11), and the frequency deviation of the new steady state is calculated by (12). The normal operation of the power system frequency is $\Delta f_{allow} = \pm 0.5\%$ [22-23]. For the case of disturbances decreasing frequency, when the system returns to a new steady-state with SSFD less than -0.5% , the second frequency control must be enabled by the TSOs to elaborate maximum power injected into the grid to restore the frequency into normal limits. If the frequency does not return to normal limits, through secondary control actions, load shedding must be deployed to prevent system blackouts. Modifying (12) to restore the frequency deviation within normal limits, the maximum power for the secondary control stage and the minimum power for load shedding can be derived as:

$$\Delta f_{allow} = \frac{(\Delta P_d + \Delta P_{secondary\ control\ max} - P_{LS\ min}) + c\Delta v_d}{(1-\alpha)D + (1-\alpha)/R + \alpha a_0} \quad (15)$$

where $\Delta P_{secondary\ control\ max}$ is the maximum power available for secondary control. The minimum power for load shedding is given as:

$$P_{LS\ min} = \Delta P_d - \Delta P_{secondary\ control\ max} - \Delta f_{allow} \left[(1-\alpha)D + \frac{1-\alpha}{R} + \alpha a_0 \right] \quad (16)$$

VI. DISTRIBUTION POWER METHOD FOR LOAD SHEDDING

The VED method can be elaborated by the following steps [24-27].

- Step 1: Convert all buses to load buses (change all PV buses into PQ buses).
- Step 2: Determine $[\partial V/\partial Q]$ in all buses. This inverse of the Jacobian matrix indicates the relationship between the reactive power injection at one bus to the voltage variation of the neighboring buses as follows:

$$\Delta V_i = -[\partial V_i/\partial Q_j] \Delta Q_j = -J_{ij}^{-1} \Delta Q_j \quad (17)$$

where, J_{ij}^{-1} is the sensitivity matrix $[\partial V_i/\partial Q_j]$.

- Step 3: Calculate α_{ij} using the sensitivity matrix in Step 2. Then the voltage variation relationship between bus i and bus j is given as:

$$\Delta V_i = [J_{ij}^{-1}/J_{jj}^{-1}] \Delta V_j = \alpha_{ij} \Delta V_j \quad (18)$$

where, α_{ij} is defined as $[J_{ij}^{-1}/J_{jj}^{-1}]$.

- Step 4: Calculate the VED using the cross product of $\alpha_{ii}(\alpha_{ij} \times \alpha_{ji})$ which is reflected by the symmetrical distance:

$$D_V(i, j) = D_V(j, i) = -\text{Log}(\alpha_{ij} \times \alpha_{ji}) \quad (19)$$

where, α_{ji} is defined as $[J_{ji}^{-1}/J_{ii}^{-1}]$.

The load shedding power is then given as [21]:

$$P_{LSi} = \frac{D_{V,eq}}{D_{V,mi}} \cdot P_{LSmin} \quad (20)$$

where P_{LSi} is the shedding power needed at bus i (MW), P_{LSmin} is the minimum power for optimal load shedding (MW), $D_{V,mi}$ is the VED value of the corresponding load bus i to the fault bus, and $D_{V,eq}$ is the equivalent VED value of all load buses to the fault bus.

In addition, the physical-electrical relationship of the buses in the system is presented by the VED values. Equation (17) shows that the closer the distance, the smaller the D_V or the larger the α_{ij} is. On the other hand, (16) evaluates the voltage interactions between buses i and j , with a higher value of α_{ij} the voltage attenuation is more severe at bus i when a disturbance occurs at bus j . Thus, when a disturbance occurs such as tripping of a generator unit, the amplitude of the voltage fluctuation near this generator is large, leading to an attenuation voltage at nodes with increasing in VED. To ensure that the voltage profile returns to its stability margin, the load shedding power at each bus can be determined on the principle that the smaller the VED, the larger the load shedding power is and vice versa. With: $D_{V(k,1)} < D_{V(k,2)} < D_{V(k,3)} < \dots < D_{V(k,n)}$, the priority in load shedding is: Load 1 \rightarrow Load 2 \rightarrow Load 3 \rightarrow ... \rightarrow Load n .

VII. CASE STUDY AND SIMULATION RESULTS

The IEEE 37-bus test system consists of 8 conventional generators and an equivalent capacity wind farm replacing the generator on bus No.28 with the name ELM345#1 to maintain

power balance. This system was used to evaluate the suggested method. The single-line diagram of the system is shown in Figure 2, where the total load capacity is 1032MW. The ratio

of wind power to the total system capacity is 15% ($\alpha=0.15$). Table I presents the parameters of conventional generators.

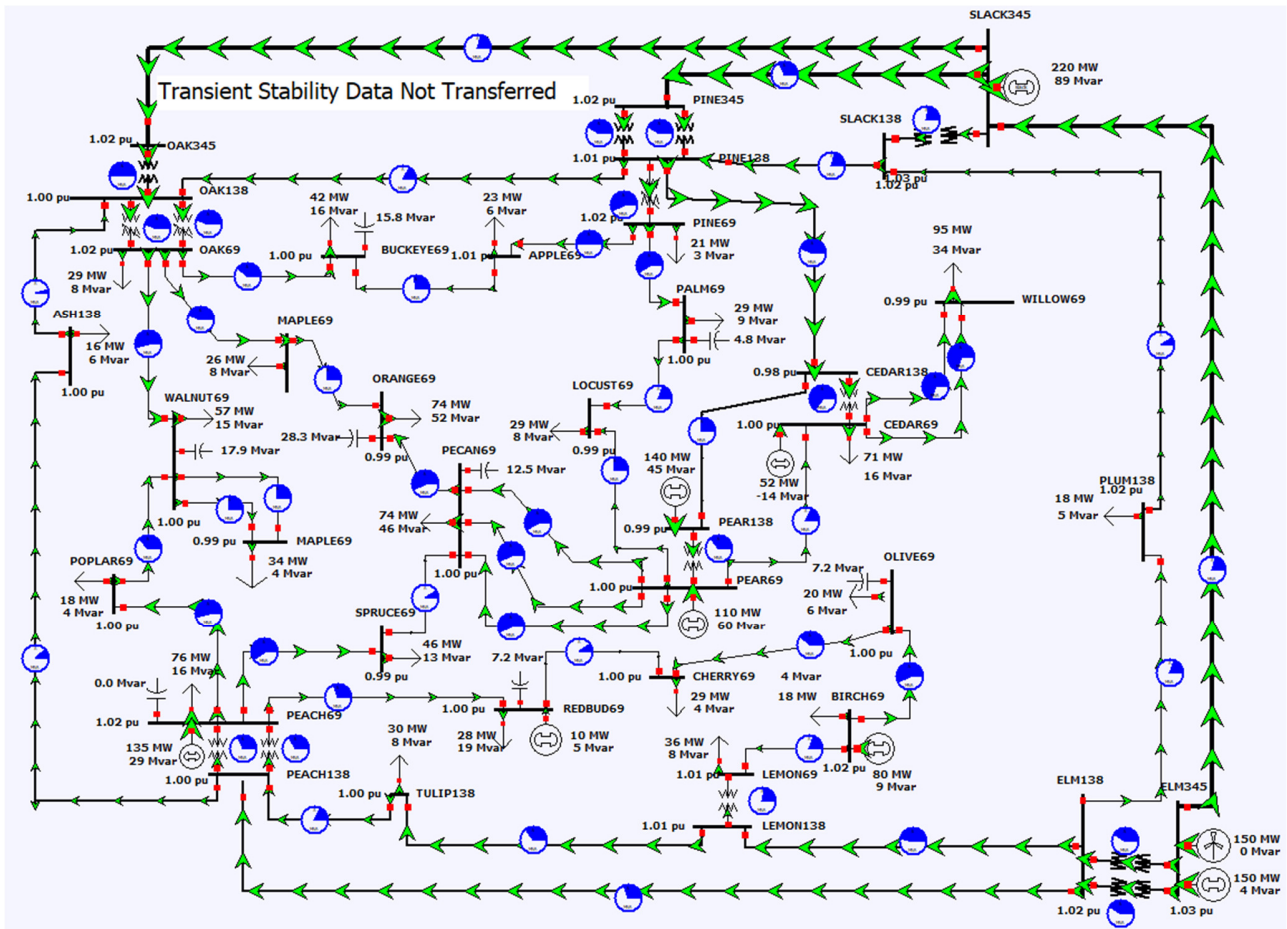


Fig. 2. The IEEE 37-Bus test system with modified wind power generator model used in the simulation.

TABLE I. PARAMETERS OF THE CONVENTIONAL GENERATORS

Bus No.	Bus name	H (s)	D	Min MW	Max MW	Min Mvar	Max Mvar
14	REDBUD69	1.328	0.848	10	35	0	5
28	ELM345#2	11.16	3.384	0	150	-60	60
31	SLACK345	18.75	6.5	0	220	-90	120
44	PEACH69	4.352	2.72	0	150	-20	40
48	CEDAR69	1.71	1.197	16	52	-14	26
50	BIRCH69	3.4	0.7905	38	80	-18	33
53	PEAR138	9.3	2.175	22	140	0	45
54	PEAR69	4.6	2.5645	15	110	-20	60

TABLE II. EQUIVALENT PARAMETERS OF THE WIND POWER PLANT

WTG	$H_w = 3$	$k_w = 0.2$	$R_w = 0.05$	$k_p = 0.73$
	$\alpha = 0.15$	$k_b = 250$	$k_c = 0.0771$	$k_\beta = -0.1422$

TABLE III. CLASSICAL POWER SYSTEM PARAMETERS

Classical power system	$R = 0.05$	$D = 1$	$T_R = 7$	$F_H = 0.3$
------------------------	------------	---------	-----------	-------------

The parameters of the equivalent converting model of the wind power plant are shown in Table II. The disturbance factor

used in the simulation is the sudden tripping of generator ELM345#2 at bus 28, which equals 14% of total power capacity ($\Delta Pu = 0.14pu$) and neglects the disturbance factor from wind speed variation ($\Delta v = 0$). Using (14), the equivalent system inertia time constant was $H = 4.60849$. Table III presents the other parameters of the traditional power system. The modified FR model was used to analyze the frequency response of the system. The initial rate of frequency change and the steady-state frequency deviation can be obtained from (11) and (12). The simulation result of the system frequency variation is shown in Figure 3.

$$IRCF = \frac{0.14}{0.15 \times 0.2 + 2(1 - 0.15) \times 4.60849} = 0.0178pu = 1.068Hz$$

$$SSFD = \frac{0.14}{(1 - 0.15) \times 1 + \frac{1 - 0.15}{0.05} + 0.15 \times 19.9165} = 0.0067pu = 0.4031Hz$$

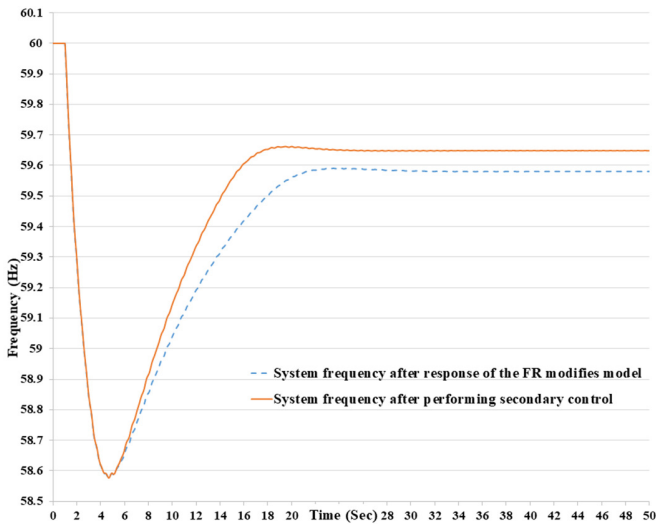


Fig. 3. The system frequency after the response of the FR modifies the model and performs secondary control.

The maximum power of the secondary control depends on the generator’s capability to inject additional power into the system. After the primary frequency control of the system applies the modified FR model, the additional power that can be transmitted to the system from each generating unit is shown in Table IV.

TABLE IV. THE CAPABILITY OF GENERATORS IN SECONDARY FREQUENCY CONTROL

Bus No.	Bus name	Status	Available power for secondary control (MW)
14	REDBUD69	Closed	17.05
28	ELM345-1	Closed	0
28	ELM345-2	Closed	0
31	SLACK345	Closed	0
44	PEACH69	Closed	0
48	CEDAR69	Closed	0
50	BIRCH69	Closed	0
53	PEAR138	Opened	0
54	PEAR69	Closed	0

Using (16), the minimum shedding power to restore the frequency within normal operating limits is calculated as:

$$\begin{aligned}
 P_{LS \min} + \Delta P_{\text{secondary control max}} &= \\
 0.14 - \frac{0.3}{60} \left[(1 - 0.15) \times 1 + \frac{1-0.15}{0.05} + 0.15 \times 19.9165 \right] &= \\
 = 0.0358 \text{ pu} = 36.96 \text{ MW} & \\
 P_{LS \min} = 36.96 - \Delta P_{\text{secondary control max}} = 36.96 - 17.05 &= \\
 = 19.91 \text{ MW} &
 \end{aligned}$$

Applying the optimum load-shedding power distribution method, the voltage electrical distance values from the load buses to the bus containing the fault generator ELM345#2 are shown in Figure 4. The shedding power at each load bus is shown in Table V.

The Under-Frequency Load Shedding (UFLS) relay method [28] was employed to evaluate the effectiveness of the

proposed method. According to [28], with an initial frequency change rate of 1.068Hz, the total load shedding capacity will be 9% of the entire system, corresponding to 92.88MW shedding power. Figure 6 presents a comparison chart of the frequency response between the conventional and the proposed method. The results show that the UFLS method has a better recovery frequency of 59.84Hz, while the proposed method has a recovery frequency of 59.7Hz. However, the shedding power of the UFLS method is higher than 72.97MW, which increases cost. This is an advantage of the proposed shedding method.

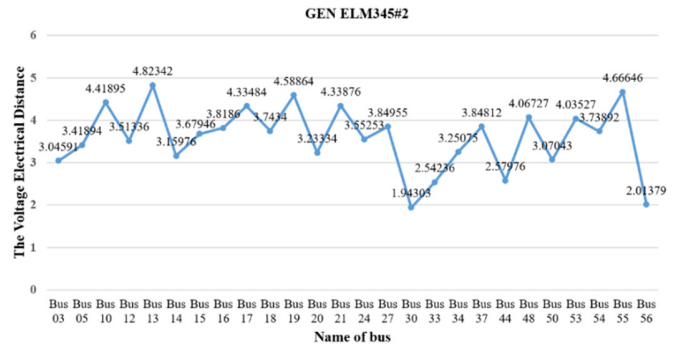


Fig. 4. The VED from ELM345#2 generator to load buses.

TABLE V. SHEDDING POWER AT EACH LOAD BUS DISTRIBUTED ACCORDING TO VOLTAGE DISTANCE

Bus No.	Load shedding power (MW)
3	0.854823
5	0.761556
10	0.589216
12	0.74109
13	0.539807
14	0.824023
15	0.707635
16	0.681851
17	0.600648
18	0.695548
19	0.567426
20	0.805271
21	0.600106
24	0.732919
27	0.676369
30	1.340028
33	1.024133
34	0.800958
37	0.67662
44	1.009286
48	0.640163
50	0.847997
53	0.645239
54	0.696382
55	0.557964
56	1.292943
Total	19.91

Figure 6 shows a comparison of the voltage magnitude with and without the use of the proposed shedding method. The results show that the steady-state voltage in load shedding is higher than without load shedding. This improvement in voltage magnitude comes from the amount of load power removed from the system. In addition, the suggested method of

distributing the shedding power to the load buses gives more selectivity than the UFLS because it is based on the VED of the fault bus to the load buses.

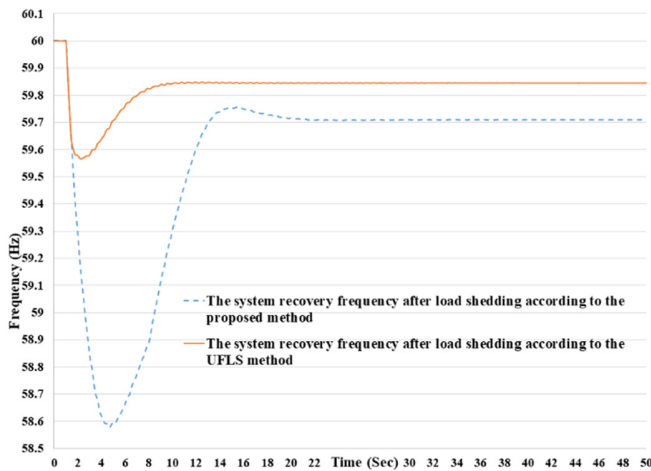


Fig. 5. The recovery frequency of the system after performing load shedding according to the proposed and the UFLS method.

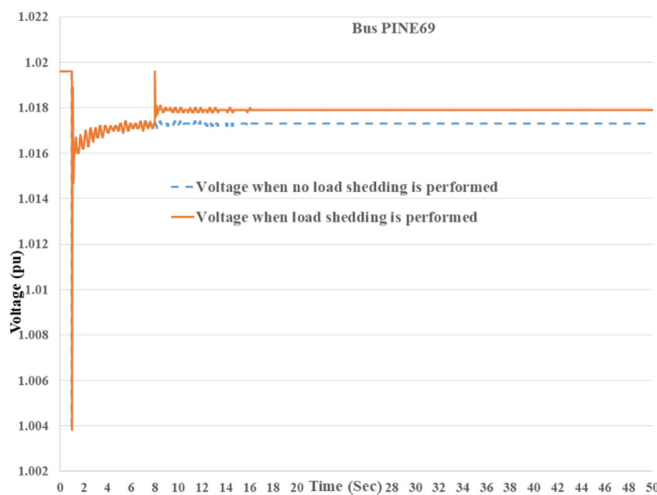


Fig. 6. Voltage comparison with load shedding based on the proposed method and no load shedding at Bus PINE69.

VIII. CONCLUSION

Applying the modified FR model to a high-integrated wind energy power system demonstrated the system's frequency response when interference occurs and proved its effectiveness. This model is suitable for a traditional power system increasingly integrated with renewable energy sources. The calculation of the minimum load shedding power considering the modified FR model and the system's secondary frequency control helped reduce power for load shedding and restore frequency to the normal operation range, lessening the impact caused by load shedding. This demonstrates the feasibility of controlling a traditional power system with the integration of renewable energy sources. The VED method was applied to distribute the shedding power to the load buses, making load shedding more selective and providing a fast recovery in the system frequency. The effectiveness of the proposed method

was evaluated through simulation on the IEEE 37-bus test system with a modified wind power generator. In the future, optimization issues for load shedding in high-integrated wind energy power systems considering costs of power generation and penalty charges from load shedding will be studied, optimization algorithms will be applied, and the rank of priority of the loads will also be taken into account.

ACKNOWLEDGMENT

This study belongs to the project with grant No: T2021-59TD funded by the Ho Chi Minh City University of Technology and Education, Vietnam.

REFERENCES

- [1] S. Eryilmaz and C. Kan, "Reliability based modeling and analysis for a wind power system integrated by two wind farms considering wind speed dependence," *Reliability Engineering & System Safety*, vol. 203, Aug. 2020, Art. no. 107077, <https://doi.org/10.1016/j.res.2020.107077>.
- [2] A. Noori, M. Jafari Shahbazadeh, and M. Eslami, "Designing of wide-area damping controller for stability improvement in a large-scale power system in presence of wind farms and SMES compensator," *International Journal of Electrical Power & Energy Systems*, vol. 119, Apr. 2020, Art. no. 105936, <https://doi.org/10.1016/j.ijepes.2020.105936>.
- [3] E. S. N. R. Paidi, H. Marzoochi, J. Yu, and V. Terzija, "Development and Validation of Artificial Neural Network-Based Tools for Forecasting of Power System Inertia With Wind Farms Penetration," *IEEE Systems Journal*, vol. 14, no. 4, pp. 4978–4989, Sep. 2020, <https://doi.org/10.1109/JSYST.2020.3017640>.
- [4] G. Qiu, J. Liu, Y. Liu, T. Liu, and G. Mu, "Ensemble Learning for Power Systems TTC Prediction With Wind Farms," *IEEE Access*, vol. 7, pp. 16572–16583, 2019, <https://doi.org/10.1109/ACCESS.2019.2896198>.
- [5] P. Wang, Z. Zhang, Q. Huang, and W.-J. Lee, "Wind Farm Dynamic Equivalent Modeling Method for Power System Probabilistic Stability Assessment," *IEEE Transactions on Industry Applications*, vol. 56, no. 3, pp. 2273–2280, Feb. 2020, <https://doi.org/10.1109/TIA.2020.2970377>.
- [6] J. Liu, Y. Xu, Z. Y. Dong, and K. P. Wong, "Retirement-Driven Dynamic VAR Planning for Voltage Stability Enhancement of Power Systems With High-Level Wind Power," *IEEE Transactions on Power Systems*, vol. 33, no. 2, pp. 2282–2291, Mar. 2018, <https://doi.org/10.1109/TPWRS.2017.2732441>.
- [7] M. Khamies, G. Magdy, S. Kamel, and B. Khan, "Optimal Model Predictive and Linear Quadratic Gaussian Control for Frequency Stability of Power Systems Considering Wind Energy," *IEEE Access*, vol. 9, pp. 116453–116474, 2021, <https://doi.org/10.1109/ACCESS.2021.3106448>.
- [8] T. Le and B. L. N. Phung, "Load Shedding in Microgrids with Consideration of Voltage Quality Improvement," *Engineering, Technology & Applied Science Research*, vol. 11, no. 1, pp. 6680–6686, Feb. 2021, <https://doi.org/10.48084/etasr.3931>.
- [9] M. A. Zdiri, A. S. Alshammari, A. A. Alzamil, M. B. Ammar, and H. H. Abdallah, "Optimal Shedding Against Voltage Collapse Based on Genetic Algorithm," *Engineering, Technology & Applied Science Research*, vol. 11, no. 5, pp. 7695–7701, Oct. 2021, <https://doi.org/10.48084/etasr.4448>.
- [10] P. D. Chung, "Retaining of Frequency in Micro-grid with Wind Turbine and Diesel Generator," *Engineering, Technology & Applied Science Research*, vol. 8, no. 6, pp. 3646–3651, Dec. 2018, <https://doi.org/10.48084/etasr.2413>.
- [11] H. Ye, W. Pei, and Z. Qi, "Analytical Modeling of Inertial and Droop Responses From a Wind Farm for Short-Term Frequency Regulation in Power Systems," *IEEE Transactions on Power Systems*, vol. 31, no. 5, pp. 3414–3423, Sep. 2016, <https://doi.org/10.1109/TPWRS.2015.2490342>.

- [12] H. Bialas, R. Pawelek, and I. Wasiak, "A Simulation Model for Providing Analysis of Wind Farms Frequency and Voltage Regulation Services in an Electrical Power System," *Energies*, vol. 14, no. 8, Jan. 2021, Art. no. 2250, <https://doi.org/10.3390/en14082250>.
- [13] G. Xu, C. Zhu, T. Bi, A. Xue, and J. Hu, "Optimal Frequency Controller Parameters of Wind Turbines Participating System Frequency Control," in *2018 IEEE Power Energy Society General Meeting (PESGM)*, Dec. 2018, pp. 1–5, <https://doi.org/10.1109/PESGM.2018.8586412>.
- [14] Y. F. Hassan, Y. G. Rashid, and F. M. Tuaimah, "Demand Priority in a Power System With Wind Power Contribution Load Shedding Scheme Based," *Journal of Engineering*, vol. 25, no. 11, pp. 92–111, 2019.
- [15] W. Gan *et al.*, "Two-Stage Planning of Network-Constrained Hybrid Energy Supply Stations for Electric and Natural Gas Vehicles," *IEEE Transactions on Smart Grid*, vol. 12, no. 3, pp. 2013–2026, Feb. 2021, <https://doi.org/10.1109/TSG.2020.3039493>.
- [16] Y. Tang, J. Dai, J. Ning, J. Dang, Y. Li, and X. Tian, "An Extended System Frequency Response Model Considering Wind Power Participation in Frequency Regulation," *Energies*, vol. 10, no. 11, Nov. 2017, Art. no. 1797, <https://doi.org/10.3390/en10111797>.
- [17] P. M. Anderson and M. Mirheydar, "A low-order system frequency response model," *IEEE Transactions on Power Systems*, vol. 5, no. 3, pp. 720–729, Dec. 1990, <https://doi.org/10.1109/59.65898>.
- [18] H. Katsuura and D. A. Sprecher, "Computational aspects of Kolmogorov's superposition theorem," *Neural Networks*, vol. 7, no. 3, pp. 455–461, Jan. 1994, [https://doi.org/10.1016/0893-6080\(94\)90079-5](https://doi.org/10.1016/0893-6080(94)90079-5).
- [19] J. Zou, C. Peng, Y. Yan, H. Zheng, and Y. Li, "A survey of dynamic equivalent modeling for wind farm," *Renewable and Sustainable Energy Reviews*, vol. 40, pp. 956–963, Sep. 2014, <https://doi.org/10.1016/j.rser.2014.07.157>.
- [20] P. Wang, Z. Zhang, Q. Huang, N. Wang, X. Zhang, and W.-J. Lee, "Improved Wind Farm Aggregated Modeling Method for Large-Scale Power System Stability Studies," *IEEE Transactions on Power Systems*, vol. 33, no. 6, pp. 6332–6342, Aug. 2018, <https://doi.org/10.1109/TPWRS.2018.2828411>.
- [21] M. Krpan and I. Kuzle, "Introducing low-order system frequency response modelling of a future power system with high penetration of wind power plants with frequency support capabilities," *IET Renewable Power Generation*, vol. 12, no. 13, pp. 1453–1461, 2018, <https://doi.org/10.1049/iet-rpg.2017.0811>.
- [22] "IEEE Guide for the Application of Protective Relays Used for Abnormal Frequency Load Shedding and Restoration," IEEE Power Engineering Society, Standard C37.117-2007, Mar. 2007.
- [23] J. H. Eto, J. Undrill, C. Roberts, P. Mackin, and J. Ellis, "Frequency Control Requirements for Reliable Interconnection Frequency Response," Energy Analysis and Environmental Impacts Division Lawrence Berkeley National Laboratory, Feb. 2018.
- [24] L. Patrick, "The different electrical distance," in *Proceedings of the Tenth Power Systems Computation Conference*, Graz, Austria, Aug. 1990, pp. 542–550.
- [25] L. T. Nghia, Q. H. Anh, P. T. T. Binh, N. T. An, and P. H. Hau, "A voltage electrical distance application for power system load shedding considering the primary and secondary generator controls," *International Journal of Electrical and Computer Engineering (IJECE)*, vol. 9, no. 5, pp. 3993–4002, Oct. 2019.
- [26] H. Nemouchi, A. Tiguercha, and A. A. Ladjici, "An adaptive decentralized under voltage load shedding in distribution networks," *International Transactions on Electrical Energy Systems*, vol. 30, no. 11, 2020, Art. no. e12592, <https://doi.org/10.1002/2050-7038.12592>.
- [27] S. H. Song, H. C. Lee, Y. T. Yoon, and S.-I. Moon, "Cluster design compatible with market for effective reactive power management," in *2006 IEEE Power Engineering Society General Meeting*, Montreal, Canada, Jun. 2006, <https://doi.org/10.1109/PES.2006.1709405>.
- [28] Florida Reliability Coordinating Council, "FRCC Regional Frequency Load Shedding (UFLS) Implementation Schedule," in *FRCC Handbook*, Jun. 2011.